

Introduction to Quantum Chromodynamics and Loop Calculations

Gudrun Heinrich

Max Planck Institute for Physics, Munich

24th Vietnam School of Physics, Quy Nhon, August 2018

Lectures 4-6

Contents

1	Quantum Chromodynamics as a non-Abelian gauge theory	2
2	Tree level amplitudes	2
3	Higher orders in perturbation theory	2
3.1	Dimensional regularisation	3
3.2	Regularisation schemes	4
3.3	One-loop integrals	5
3.4	Renormalisation	14
3.5	The running coupling and the QCD beta function	15
3.6	NLO calculations and infrared singularities	20
3.6.1	Structure of NLO calculations	20
3.6.2	Soft gluon emission and collinear singularities	23
3.6.3	Phase space integrals in D dimensions	23
3.6.4	Jet cross sections	25
3.7	Parton distribution functions	31

1 Quantum Chromodynamics as a non-Abelian gauge theory

See lectures 1 and 2.

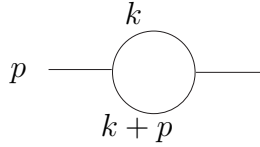
2 Tree level amplitudes

See lecture 3.

3 Higher orders in perturbation theory

Tree level results in QCD are mostly not accurate enough to match the current experimental precision and suffer from large scale uncertainties. When calculating higher orders, we will encounter singularities: ultraviolet (UV) singularities, and infrared (IR) singularities due to soft or collinear massless particles. Therefore the introduction of a *regulator* is necessary.

Let us first have a look at UV singularities: The expression for the one-loop two-point function shown below naively would be



$$I_2 = \int_{-\infty}^{\infty} \frac{d^4 k}{(2\pi)^4} \frac{1}{[k^2 - m^2 + i\delta][(k+p)^2 - m^2 + i\delta]} . \quad (3.1)$$

If we are only interested in the behaviour of the integral for $|k| \rightarrow \infty$ we can neglect the masses, transform to polar coordinates and obtain

$$I_2 \sim \int d\Omega_3 \int_0^{\infty} d|k| \frac{|k|^3}{|k|^4} . \quad (3.2)$$

This integral is clearly not well-defined. If we introduce an upper cutoff Λ (and a lower limit $|k|_{\min}$ because we neglected the masses and p^2) it is regulated:

$$I_2 \sim \int_{|k|_{\min}}^{\Lambda} d|k| \frac{1}{|k|} \sim \log \Lambda . \quad (3.3)$$

The integral has a logarithmic UV divergence. The problem with the regulator Λ is that it is neither Lorentz invariant nor gauge invariant. A regularisation method which preserves the symmetries is dimensional regularisation.

3.1 Dimensional regularisation

Dimensional regularisation has been introduced in 1972 by 't Hooft and Veltman [1] (and by Bollini and Giambiagi [2]) as a method to regularise UV divergences in a gauge invariant way, thus completing the proof of renormalisability.

The idea is to work in $D = 4 - 2\epsilon$ space-time dimensions. This means that the Lorentz algebra objects (momenta, polarisation vectors, metric tensor) live in a D -dimensional space. The γ -algebra also has to be extended to D dimensions. Divergences for $D \rightarrow 4$ will appear as poles in $1/\epsilon$.

An important feature of dimensional regularisation is that it regulates IR singularities, i.e. soft and/or collinear divergences due to massless particles, as well. Ultraviolet divergences occur if the loop momentum $k \rightarrow \infty$, so in general the UV behaviour becomes better for $\epsilon > 0$, while the IR behaviour becomes better for $\epsilon < 0$. Certainly we cannot have $D < 4$ and $D > 4$ at the same time. What is formally done is to first assume the IR divergences are regulated in some other way, e.g. by assuming all external legs are off-shell or by introducing a small mass for all massless particles. In this case all poles in $1/\epsilon$ will be of UV nature and renormalisation can be performed. Then we can analytically continue to the whole complex D -plane, in particular to $\text{Re}(D) > 4$. If we now remove the auxiliary IR regulator, the IR divergences will show up as $1/\epsilon$ poles. (This is however not done in practice, where all poles just show up as $1/\epsilon$ poles, and after UV renormalisation, the remaining ones must be of IR nature.)

The only change to the Feynman rules to be made is to replace the couplings in the Lagrangian $g \rightarrow g\mu^\epsilon$, where μ is an arbitrary mass scale. This ensures that each term in the Lagrangian has the correct mass dimension.

The momentum integration involves $\int \frac{d^D k}{(2\pi)^D}$ for each loop, which can also be considered as an addition to the Feynman rules.

Further, each closed fermion loop and ghost loop needs to be multiplied by a factor of (-1) due to Fermi statistics.

D -dimensional γ -algebra

Extending the Clifford algebra to D dimensions implies

$$\{\gamma^\mu, \gamma^\nu\} = 2g^{\mu\nu} \quad \text{with} \quad g_\mu^\mu = D, \quad (3.4)$$

leading for example to $\gamma_\mu \not{p} \gamma^\mu = (2 - D) \not{p}$. However, it is not obvious how to continue the Dirac matrix γ_5 to D dimensions. In 4 dimensions it is defined as

$$\gamma_5 = i \gamma_0 \gamma_1 \gamma_2 \gamma_3 \quad (3.5)$$

which is an intrinsically 4-dimensional definition. In 4 dimensions, γ_5 has the algebraic properties $\gamma_5^2 = 1$, $\{\gamma_\mu, \gamma_5\} = 0$, $\text{Tr}(\gamma_\mu \gamma_\nu \gamma_\rho \gamma_\sigma \gamma_5) = 4i\epsilon_{\mu\nu\rho\sigma}$. However, in D dimensions, the latter two conditions cannot be maintained simultaneously. This can be seen by considering the expression

$$\epsilon^{\mu\nu\rho\sigma} \text{Tr}(\gamma_\tau \gamma_\mu \gamma_\nu \gamma_\rho \gamma_\sigma \gamma^\tau \gamma_5)$$

(remember $\epsilon_{\mu\nu\rho\sigma} = 1$ if $(\mu\nu\rho\sigma)$ is an even permutation of (0123) , -1 if $(\mu\nu\rho\sigma)$ is an odd permutation of (0123) and 0 otherwise). Using the cyclicity of the trace and $\{\gamma_\mu, \gamma_5\} = 0$ leads to

$$(D - 4) \epsilon^{\mu\nu\rho\sigma} \text{Tr}(\gamma_\mu \gamma_\nu \gamma_\rho \gamma_\sigma \gamma_5) = 0. \quad (3.6)$$

For $D \neq 4$ we therefore conclude that the trace must be zero, and there is no smooth limit $D \rightarrow 4$ which reproduces the non-zero trace at $D = 4$.

The most commonly used prescription [1, 3, 4] for γ_5 is to define

$$\gamma_5 = \frac{i}{4!} \epsilon_{\mu_1 \mu_2 \mu_3 \mu_4} \gamma^{\mu_1} \gamma^{\mu_2} \gamma^{\mu_3} \gamma^{\mu_4}, \quad (3.7)$$

where the Lorentz indices of the “ordinary” γ -matrices will be contracted in D dimensions. Doing so, Ward identities relying on $\{\gamma_5, \gamma_\mu\} = 0$ break down due to an extra $(D - 4)$ -dimensional contribution. These need to be repaired by so-called “finite renormalisation” terms [4]. For practical calculations it can be convenient to split the other Dirac matrices into a 4-dimensional and a $(D - 4)$ -dimensional part, $\gamma_\mu = \bar{\gamma}_\mu + \tilde{\gamma}_\mu$, where $\bar{\gamma}_\mu$ is 4-dimensional and $\tilde{\gamma}_\mu$ is $(D - 4)$ -dimensional. The definition (3.7) implies

$$\{\gamma^\mu, \gamma_5\} = \begin{cases} 0 & \mu \in \{0, 1, 2, 3\} \\ 2\tilde{\gamma}^\mu \gamma_5 & \text{otherwise.} \end{cases}$$

The second line above can also be read as $[\gamma_5, \tilde{\gamma}^\mu] = 0$, which can be interpreted as γ_5 acting trivially in the non-physical dimensions. There are other prescriptions for γ_5 , which maintain $\{\gamma_\mu^{(D)}, \gamma_5\} = 0$, but then have to give up the cyclicity of the trace.

3.2 Regularisation schemes

Related to the γ_5 -problem, it is not uniquely defined how we continue the Dirac-algebra to D dimensions. The three main schemes are:

- **CDR** (“Conventional dimensional regularisation”): Both internal and external gluons (and other vector fields) are all treated as D -dimensional.
- **HV** (“’t Hooft Veltman scheme”): Internal gluons are treated as D -dimensional but external ones are treated as 4-dimensional.

	CDR	HV	DRED
internal gluon	$g^{\mu\nu}$	$g^{\mu\nu}$	$\bar{g}^{\mu\nu}$
external gluon	$g^{\mu\nu}$	$\bar{g}^{\mu\nu}$	$\bar{g}^{\mu\nu}$

Table 1: Treatment of internal and external gluons in the different schemes.

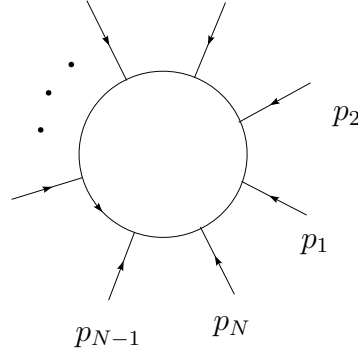
- **DRED** (“Dimensional reduction”): Internal and external gluons are treated as 4-dimensional (but not the loop integrals).

At one loop, **CDR** and **HV** are equivalent, as terms of order ϵ in external momenta do not play a role. The transition formulae to relate results obtained in one scheme to another scheme are well known at one loop [5, 6]. The conventions are summarised in Table 1.

3.3 One-loop integrals

Integration in D dimensions

Consider a generic one-loop diagram with N external legs and N propagators. If k is the loop momentum, the propagators are $q_a = k + r_a$, where $r_a = \sum_{i=1}^a p_i$. If we define all momenta as incoming, momentum conservation implies $\sum_{i=1}^N p_i = 0$ and hence $r_N = 0$.



If the vertices in the diagram above are non-scalar, this diagram will contain a Lorentz tensor structure in the numerator, leading to tensor integrals of the form

$$I_N^{D, \mu_1 \dots \mu_r}(S) = \int_{-\infty}^{\infty} \frac{d^D k}{i\pi^{\frac{D}{2}}} \frac{k^{\mu_1} \dots k^{\mu_r}}{\prod_{i \in S} (q_i^2 - m_i^2 + i\delta)}, \quad (3.8)$$

but we will first consider the scalar integral only, i.e. the case where the numerator is equal to one. S is the set of propagator labels, which can be used to characterise the integral, in our example $S = \{1, \dots, N\}$.

We use the integration measure $d^D k / i\pi^{\frac{D}{2}} \equiv d\kappa$ to avoid ubiquitous factors of $i\pi^{\frac{D}{2}}$ which will arise upon momentum integration.

Feynman parameters

To combine products of denominators of the type $d_i^{\nu_i} = [(k + r_i)^2 - m_i^2 + i\delta]^{\nu_i}$ into one single denominator, we can use the identity

$$\frac{1}{d_1^{\nu_1} d_2^{\nu_2} \dots d_N^{\nu_N}} = \frac{\Gamma(\sum_{i=1}^N \nu_i)}{\prod_{i=1}^N \Gamma(\nu_i)} \int_0^\infty \prod_{i=1}^N dz_i z_i^{\nu_i-1} \frac{\delta(1 - \sum_{j=1}^N z_j)}{[z_1 d_1 + z_2 d_2 + \dots + z_N d_N]^{\sum_{i=1}^N \nu_i}} \quad (3.9)$$

The integration parameters z_i are called *Feynman parameters*. For generic one-loop diagrams we have $\nu_i = 1 \forall i$. The propagator powers ν_i are also called *indices*.

An alternative to Feynman parametrisation is the so-called ‘‘Schwinger parametrisation’’, based on

$$\frac{1}{A^\nu} = \frac{1}{\Gamma(\nu)} \int_0^\infty dx x^{\nu-1} \exp(-x A), \quad \text{Re}(A) > 0. \quad (3.10)$$

In this case the Gaussian integration formula

$$\int_{-\infty}^\infty d^D r_E \exp(-\alpha r_E^2) = \left(\frac{\pi}{\alpha}\right)^{\frac{D}{2}}, \quad \alpha > 0 \quad (3.11)$$

is used to integrate over the momenta.

Simple example: one-loop two-point function

For $N = 2$, the corresponding 2-point integral (‘‘bubble’’) is given by

$$\begin{aligned} I_2 &= \int_{-\infty}^\infty d\kappa \frac{1}{[k^2 - m^2 + i\delta][(k+p)^2 - m^2 + i\delta]} \\ &= \Gamma(2) \int_0^\infty dz_1 dz_2 \int_{-\infty}^\infty d\kappa \frac{\delta(1 - z_1 - z_2)}{[z_1(k^2 - m^2) + z_2((k+p)^2 - m^2) + i\delta]^2} \\ &= \Gamma(2) \int_0^1 dz_2 \int_{-\infty}^\infty d\kappa \frac{1}{[k^2 + 2k \cdot Q + A + i\delta]^2} \\ Q^\mu &= z_2 p^\mu, \quad A = z_2 p^2 - m^2. \end{aligned} \quad (3.12)$$

How to do the D -dimensional momentum integration will be shown below for a general one-loop integral. The procedure also extends to multi-loop integrals and is completely straightforward. The tricky bit is usually the integration over the Feynman parameters.

Momentum integration for scalar one-loop N -point integrals

The one-loop N -point integral with rank $r = 0$ (“scalar integral”) defined in Eq. (3.8), after Feynman parametrisation, with all propagator powers $\nu_i = 1$, is of the following form

$$I_N^D = \Gamma(N) \int_0^\infty \prod_{i=1}^N dz_i \delta(1 - \sum_{l=1}^N z_l) \int_{-\infty}^\infty d\kappa \left[k^2 + 2k \cdot Q + \sum_{i=1}^N z_i (r_i^2 - m_i^2) + i\delta \right]^{-N}$$

$$Q^\mu = \sum_{i=1}^N z_i r_i^\mu . \quad (3.13)$$

Now we perform the shift $l = k + Q$ to eliminate the term linear in k in the square bracket to arrive at

$$I_N^D = \Gamma(N) \int_0^\infty \prod_{i=1}^N dz_i \delta(1 - \sum_{l=1}^N z_l) \int_{-\infty}^\infty \frac{d^D l}{i\pi^{\frac{D}{2}}} [l^2 - R^2 + i\delta]^{-N} \quad (3.14)$$

The general form of R^2 is

$$\begin{aligned} R^2 &= Q^2 - \sum_{i=1}^N z_i (r_i^2 - m_i^2) \\ &= \sum_{i,j=1}^N z_i z_j r_i \cdot r_j - \frac{1}{2} \sum_{i=1}^N z_i (r_i^2 - m_i^2) \sum_{j=1}^N z_j - \frac{1}{2} \sum_{j=1}^N z_j (r_j^2 - m_j^2) \sum_{i=1}^N z_i \\ &= -\frac{1}{2} \sum_{i,j=1}^N z_i z_j (r_i^2 + r_j^2 - 2 r_i \cdot r_j - m_i^2 - m_j^2) \\ &= -\frac{1}{2} \sum_{i,j=1}^N z_i z_j \mathcal{S}_{ij} \\ \mathcal{S}_{ij} &= (r_i - r_j)^2 - m_i^2 - m_j^2 \end{aligned} \quad (3.15)$$

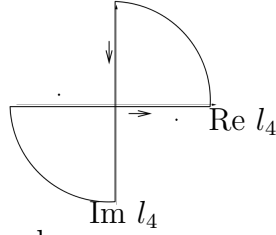
The matrix \mathcal{S}_{ij} , sometimes also called *Cayley matrix* is an important quantity encoding all the kinematic dependence of the integral. It plays a major role in the algebraic reduction of tensor integrals or integrals with higher N to simpler objects, as well as in the analysis of so-called *Landau singularities*, which are singularities where $\det \mathcal{S}$ or a sub-determinant of \mathcal{S} is vanishing (see below for more details).

Remember that we are in Minkowski space, where $l^2 = l_0^2 - \vec{l}^2$, so temporal and spatial components are not on equal footing. Note that the poles of the denominator

in Eq. (3.14) are located at $l_0^2 = R^2 + \vec{l}^2 - i\delta \Rightarrow l_0^\pm \simeq \pm\sqrt{R^2 + \vec{l}^2} \mp i\delta$. Thus the $i\delta$ term shifts the poles away from the real axis in the l_0 -plane.

For the integration over the loop momentum, we better work in Euclidean space where $l_E^2 = \sum_{i=1}^D l_i^2$. Hence we make the transformation $l_0 \rightarrow i l_4$, such that $l^2 \rightarrow -l_E^2 = l_4^2 + \vec{l}^2$, which implies that the integration contour in the complex l_0 -plane is rotated by 90° such that the contour in the complex l_4 -plane looks as shown below. This is called *Wick rotation*. We see that the $i\delta$ prescription is exactly such that the contour does not enclose any poles. Therefore the integral over the closed contour is zero, and we can use the identity

$$\int_{-\infty}^{\infty} dl_0 f(l_0) = - \int_{i\infty}^{-i\infty} dl_0 f(l_0) = i \int_{-\infty}^{\infty} dl_4 f(l_4) \quad (3.16)$$



Our integral now reads

$$I_N^D = (-1)^N \Gamma(N) \int_0^\infty \prod_{i=1}^N dz_i \delta(1 - \sum_{l=1}^N z_l) \int_{-\infty}^\infty \frac{d^D l_E}{\pi^{\frac{D}{2}}} [l_E^2 + R^2 - i\delta]^{-N} \quad (3.17)$$

Now we can introduce polar coordinates in D dimensions to evaluate the momentum integral.

$$\int_{-\infty}^\infty d^D l = \int_0^\infty dr r^{D-1} \int d\Omega_{D-1}, \quad r = \sqrt{l_E^2} = \left(\sum_{i=1}^4 l_i^2 \right)^{\frac{1}{2}} \quad (3.18)$$

$$\int d\Omega_{D-1} = V(D) = \frac{2\pi^{\frac{D}{2}}}{\Gamma(\frac{D}{2})} \quad (3.19)$$

where $V(D)$ is the volume of a unit sphere in D dimensions:

$$V(D) = \int_0^{2\pi} d\theta_1 \int_0^\pi d\theta_2 \sin \theta_2 \dots \int_0^\pi d\theta_{D-1} (\sin \theta_{D-1})^{D-2}.$$

Thus we have

$$I_N^D = 2(-1)^N \frac{\Gamma(N)}{\Gamma(\frac{D}{2})} \int_0^\infty \prod_{i=1}^N dz_i \delta(1 - \sum_{l=1}^N z_l) \int_0^\infty dr r^{D-1} \frac{1}{[r^2 + R^2 - i\delta]^N}$$

Substituting $r^2 = x$:

$$\int_0^\infty dr r^{D-1} \frac{1}{[r^2 + R^2 - i\delta]^N} = \frac{1}{2} \int_0^\infty dx x^{D/2-1} \frac{1}{[x + R^2 - i\delta]^N} \quad (3.20)$$

Now the x -integral can be identified as the Euler Beta-function $B(a, b)$, defined as

$$B(a, b) = \int_0^\infty dz \frac{z^{a-1}}{(1+z)^{a+b}} = \int_0^1 dy y^{a-1} (1-y)^{b-1} = \frac{\Gamma(a)\Gamma(b)}{\Gamma(a+b)} \quad (3.21)$$

and after normalising with respect to R^2 we finally arrive at

$$I_N^D = (-1)^N \Gamma(N - \frac{D}{2}) \int_0^\infty \prod_{i=1}^N dz_i \delta(1 - \sum_{l=1}^N z_l) [R^2 - i\delta]^{\frac{D}{2}-N} . \quad (3.22)$$

The integration over the Feynman parameters remains to be done, but for one-loop applications, the integrals we need to know explicitly have maximally $N = 4$ external legs. Integrals with $N > 4$ can be expressed in terms of boxes, triangles, bubbles and tadpoles (in the case of massive propagators). The analytic expressions for these “master integrals” are well-known. The most complicated analytic functions which can appear at one loop are dilogarithms.

The generic form of the derivation above makes clear that we do not have to go through the procedure of Wick rotation explicitly each time. All we need (for scalar integrals) is to use the following general formula for D -dimensional momentum integration (in Minkowski space, and after having performed the shift to have a quadratic form in the denominator):

$$\int \frac{d^D l}{i\pi^{\frac{D}{2}}} \frac{(l^2)^r}{[l^2 - R^2 + i\delta]^N} = (-1)^{N+r} \frac{\Gamma(r + \frac{D}{2})\Gamma(N - r - \frac{D}{2})}{\Gamma(\frac{D}{2})\Gamma(N)} [R^2 - i\delta]^{r-N+\frac{D}{2}} \quad (3.23)$$

Example one-loop two-point function

Applying the above procedure to our two-point function, we obtain

$$I_2 = \Gamma(2) \int_0^1 dz \int_{-\infty}^\infty \frac{d^D l}{i\pi^{\frac{D}{2}}} \frac{1}{[l^2 - R^2 + i\delta]^2} \quad (3.24)$$

$$R^2 = Q^2 - A = -p^2 z(1-z) + m^2 \Rightarrow$$

$$I_2 = \Gamma(2 - \frac{D}{2}) \int_0^1 dz [-p^2 z(1-z) + m^2 - i\delta]^{\frac{D}{2}-2} . \quad (3.25)$$

For $m^2 = 0$, the result can be expressed in terms of Γ -functions:

$$I_2 = (-p^2)^{\frac{D}{2}-2} \Gamma(2 - D/2) B(D/2 - 1, D/2 - 1) , \quad (3.26)$$

where the $B(a, b)$ is defined in Eq. (3.21). The two-point function has an UV pole which is contained in

$$\Gamma(2 - D/2) = \Gamma(\epsilon) = \frac{1}{\epsilon} - \gamma_E + \mathcal{O}(\epsilon) , \quad (3.27)$$

where γ_E is “Euler’s constant”, $\gamma_E = \lim_{n \rightarrow \infty} \left(\sum_{j=1}^n \frac{1}{j} - \ln n \right) = 0.5772156649 \dots$

Including the factor $g^2 \mu^{2\epsilon}$ which usually comes with the loop, and multiplying by $\frac{i\pi^{\frac{D}{2}}}{(2\pi)^D}$ for the normalisation conventions, we obtain

$$g^2 \mu^{2\epsilon} I_2 = (4\pi)^\epsilon i \frac{g^2}{(4\pi)^2} \Gamma(\epsilon) (-p^2/\mu^2)^{-\epsilon} B(1 - \epsilon, 1 - \epsilon) . \quad (3.28)$$

Useful to know:

- As the combination $\Delta = \frac{1}{\epsilon} - \gamma_E + \ln(4\pi)$ always occurs in combination with a pole, in the so-called $\overline{\text{MS}}$ subtraction scheme (“modified Minimal Subtraction”), the whole combination Δ is subtracted in the renormalisation procedure.
- Scaleless integrals (i.e. integrals containing no dimensionful scale like masses or external momenta) are zero in dimensional regularisation, more precisely:

$$\int_{-\infty}^{\infty} \frac{d^D k}{k^{2\rho}} = i\pi V(D) \delta(\rho - D/2) . \quad (3.29)$$

- If we use dimension splitting into $2m$ integer dimensions and the remaining 2ϵ -dimensional space, $k_{(D)}^2 = k_{(2m)}^2 + \tilde{k}_{(-2\epsilon)}^2$, we will encounter additional integrals with powers of $(\tilde{k}^2)^\alpha$ in the numerator. These are related to integrals in higher dimensions by

$$\int \frac{d^D k}{i\pi^{\frac{D}{2}}} (\tilde{k}^2)^\alpha f(k^\mu, k^2) = (-1)^\alpha \frac{\Gamma(\alpha + \frac{D}{2} - 2)}{\Gamma(\frac{D}{2} - 2)} \int \frac{d^{D+2\alpha} k}{i\pi^{\frac{D}{2} + \alpha}} f(k^\mu, k^2) . \quad (3.30)$$

Note that $1/\Gamma(\frac{D}{2} - 2)$ is of order ϵ . Therefore the integrals with $\alpha > 0$ only contribute if the k -integral in $4 - 2\epsilon + 2\alpha$ dimensions is divergent. In this case they contribute a part which cannot contain a logarithm or dilogarithm (because it is the coefficient of an UV pole at one loop), so must be a rational function of the invariants involved (masses, kinematic invariants s_{ij}). Such contributions form part of the so-called “rational part” of the full amplitude.

Tensor integrals

If we have loop momenta in the numerator, as in eq. (3.8) for $r > 0$, the integration procedure is essentially the same, except for combinatorics and additional Feynman parameters in the numerator. The substitution $k = l - Q$ introduces terms of the form $(l - Q)^{\mu_1} \dots (l - Q)^{\mu_r}$ into the numerator of eq. (3.14). As the denominator is symmetric under $l \rightarrow -l$, only the terms with even numbers of l^μ in the numerator will give a non-vanishing contribution upon l -integration. Further, we know that integrals where the Lorentz structure is only carried by loop momenta, but not by external momenta, can only be proportional to combinations of metric tensors $g^{\mu\nu}$. Therefore we have, as the tensor-generalisation of eq. (3.23),

$$\int_{-\infty}^{\infty} \frac{d^D l}{i\pi^{\frac{D}{2}}} \frac{l^{\mu_1} \dots l^{\mu_{2m}}}{[l^2 - R^2 + i\delta]^N} = (-1)^N [(g^{\cdot\cdot})^{\otimes m}]^{\{\mu_1 \dots \mu_{2m}\}} \left(-\frac{1}{2}\right)^m \frac{\Gamma(N - \frac{D+2m}{2})}{\Gamma(N)} (R^2 - i\delta)^{-N+(D+2m)/2}, \quad (3.31)$$

which can be derived for example by taking derivatives of the unintegrated scalar expression with respect to l^μ . $(g^{\cdot\cdot})^{\otimes m}$ denotes m occurrences of the metric tensor and the sum over all possible distributions of the $2m$ Lorentz indices μ_i to the metric tensors is denoted by $[\dots]^{\{\mu_1 \dots \mu_{2m}\}}$. Thus, for a general tensor integral, working out the numerators containing the combinations of external vectors Q^μ , one finds the following formula:

$$I_N^{D, \mu_1 \dots \mu_r} = \sum_{m=0}^{\lfloor r/2 \rfloor} \left(-\frac{1}{2}\right)^m \sum_{j_1, \dots, j_{r-2m}=1}^{N-1} [(g^{\cdot\cdot})^{\otimes m} r_{j_1}^{\cdot\cdot} \dots r_{j_{r-2m}}^{\cdot\cdot}]^{\{\mu_1 \dots \mu_r\}} I_N^{D+2m}(j_1, \dots, j_{r-2m}) \quad (3.32)$$

$$I_N^d(j_1, \dots, j_\alpha) = (-1)^N \Gamma(N - \frac{d}{2}) \int \prod_{i=1}^N dz_i \delta(1 - \sum_{l=1}^N z_l) z_{j_1} \dots z_{j_\alpha} (R^2 - i\delta)^{d/2-N} \quad (3.33)$$

$$R^2 = -\frac{1}{2} z \cdot \mathcal{S} \cdot z$$

The distribution of the r Lorentz indices μ_i to the external vectors $r_j^{\mu_i}$ is denoted by $[\dots]^{\{\mu_1 \dots \mu_r\}}$. These are $\binom{r}{2m} \prod_{k=1}^m (2k-1)$ terms. $(g^{\cdot\cdot})^{\otimes m}$ denotes m occurrences of the metric tensor and $\lfloor r/2 \rfloor$ is the nearest integer less or equal to $r/2$. Integrals with $z_{j_1} \dots z_{j_\alpha}$ in eq. (3.33) are associated with external vectors $r_{j_1} \dots r_{j_\alpha}$, stemming from factors of Q^μ in eq. (3.14).

How the higher dimensional integrals I_N^{D+2m} in eq. (3.32), associated with metric tensors $(g^{\cdot\cdot})^{\otimes m}$, arise, is left as an exercise.

Form factor representation

A *form factor representation* of a tensor integral (or a tensor in general) is a representation where the Lorentz structure has been extracted, each Lorentz tensor multiplying a scalar quantity, the *form factor*. Distinguishing A, B, C depending on the presence of zero, one or two metric tensors, we can write

$$\begin{aligned}
I_N^{D, \mu_1 \dots \mu_r}(S) = & \sum_{j_1 \dots j_r \in S} r_{j_1}^{\mu_1} \dots r_{j_r}^{\mu_r} A_{j_1 \dots j_r}^{N, r}(S) \\
& + \sum_{j_1 \dots j_{r-2} \in S} [g^{\cdot\cdot} r_{j_1}^{\cdot} \dots r_{j_{r-2}}^{\cdot}]^{\{\mu_1 \dots \mu_r\}} B_{j_1 \dots j_{r-2}}^{N, r}(S) \\
& + \sum_{j_1 \dots j_{r-4} \in S} [g^{\cdot\cdot} g^{\cdot\cdot} r_{j_1}^{\cdot} \dots r_{j_{r-4}}^{\cdot}]^{\{\mu_1 \dots \mu_r\}} C_{j_1 \dots j_{r-4}}^{N, r}(S) .
\end{aligned} \tag{3.34}$$

Example for the distribution of indices:

$$\begin{aligned}
I_N^{D, \mu_1 \mu_2 \mu_3}(S) = & \sum_{l_1, l_2, l_3 \in S} r_{l_1}^{\mu_1} r_{l_2}^{\mu_2} r_{l_3}^{\mu_3} A_{l_1 l_2 l_3}^{N, 3}(S) \\
& + \sum_{l \in S} (g^{\mu_1 \mu_2} r_l^{\mu_3} + g^{\mu_1 \mu_3} r_l^{\mu_2} + g^{\mu_2 \mu_3} r_l^{\mu_1}) B_l^{N, 3}(S) .
\end{aligned}$$

Note that we never need more than two metric tensors in a gauge where the rank $r \leq N$. Three metric tensors would be needed for rank six, and with the restriction $r \leq N$, rank six could only be needed for six-point integrals or higher. However, we can immediately reduce integrals with $N > 5$ to lower-point ones, because for $N \geq 6$ we have the relation

$$I_N^{D, \mu_1 \dots \mu_r}(S) = - \sum_{j \in S} \mathcal{C}_j^{\mu_1} I_{N-1}^{D, \mu_2 \dots \mu_r}(S \setminus \{j\}) \quad (N \geq 6) , \tag{3.35}$$

where $\mathcal{C}_l^\mu = \sum_{k \in S} (\mathcal{S}^{-1})_{kl} r_k^\mu$ if \mathcal{S} is invertible (and if not, it can be constructed from the pseudo-inverse [7, 8]). The fact that integrals with $N \geq 6$ can be reduced to lower-point ones so easily (without introducing higher dimensional integrals) is related to the fact that in 4 space-time dimensions, we can have maximally 4 independent external momenta, the additional external momenta must be linearly dependent on the 4 ones picked to span Minkowski space. (Note that for $N = 5$ we can eliminate one external momentum by momentum conservation, to be left with 4 independent ones in 4 dimensions.) In D dimensions there is a subtlety, this is why the case $N = 5$ is

special:

$$I_5^D(S) = \sum_{j \in S} b_j \left(I_4^D(S \setminus \{j\}) - (4 - D) I_5^{D+2}(S) \right), \quad (3.36)$$

with $b_j = \sum_{k \in S} (\mathcal{S}^{-1})_{kj}$. As $4 - D = 2\epsilon$ and I_5^{D+2} is always finite, the second term can be dropped for one-loop applications. Similar for pentagon tensor integrals [7].

Historically, tensor integrals occurring in one-loop amplitudes were reduced to scalar integrals using so-called *Passarino-Veltman* reduction [9]. It is based on the fact that at one loop, scalar products of loop momenta with external momenta can always be expressed as combinations of propagators. The problem with Passarino-Veltman reduction is that it introduces powers of inverse Gram determinants $1/(\det G)^r$ for the reduction of a rank r tensor integral. This can lead to numerical instabilities upon phase space integration in kinematic regions where $\det G \rightarrow 0$.

Example for *Passarino-Veltman reduction*:

Consider a rank one three-point integral

$$I_3^{D,\mu}(S) = \int_{-\infty}^{\infty} d\bar{k} \frac{k^\mu}{[k^2 + i\delta][(k + p_1)^2 + i\delta][(k + p_1 + p_2)^2 + i\delta]} = A_1 r_1^\mu + A_2 r_2^\mu$$

$r_1 = p_1, r_2 = p_1 + p_2.$

Contracting with r_1 and r_2 and using the identities

$$k \cdot r_i = \frac{1}{2} [(k + r_i)^2 - k^2 - r_i^2], \quad i \in \{1, 2\}$$

we obtain, after cancellation of numerators

$$\begin{pmatrix} 2r_1 \cdot r_1 & 2r_1 \cdot r_2 \\ 2r_2 \cdot r_1 & 2r_2 \cdot r_2 \end{pmatrix} \begin{pmatrix} A_1 \\ A_2 \end{pmatrix} = \begin{pmatrix} R_1 \\ R_2 \end{pmatrix} \quad (3.37)$$

$$R_1 = I_2^D(r_2) - I_2^D(r_2 - r_1) - r_1^2 I_3(r_1, r_2)$$

$$R_2 = I_2^D(r_1) - I_2^D(r_2 - r_1) - r_2^2 I_3(r_1, r_2).$$

We see that the solution involves the inverse of the Gram matrix $G_{ij} = 2r_i \cdot r_j$.

Libraries where the scalar integrals and tensor one-loop form factors can be obtained numerically:

- LoopTools [10, 11]
- OneLoop [12]

- `golem95` [13–15]
- `Collier` [16]
- `Package-X` [17]

Scalar integrals only: `QCDLoop` [18, 19].

The calculation of one-loop amplitudes with many external legs is most efficiently done using “unitarity-cut-inspired” methods, for a review see Ref. [20]. One of the advantages is that it allows (numerical) reduction at *integrand level* (rather than integral level), which helps to avoid the generation of spurious terms which blow up intermediate expressions before gauge cancellations come into action.

3.4 Renormalisation

We have seen already how UV divergences can arise and how to regularize them. The procedure to absorb the divergences into a re-definition of parameters and fields is called *renormalisation*. How to deal with the finite parts defines the *renormalisation scheme*. Physical observables cannot depend on the chosen renormalisation scheme (but remember that for example the top quark mass is not an observable, so the value for the top quark mass is scheme dependent).

As QCD is renormalisable, the renormalisation procedure does not change the structure of the interactions present at tree level. The renormalised Lagrangian is obtained by rewriting the “bare” Lagrangian in terms of renormalised fields as

$$\mathcal{L}(A_0, q_0, \eta_0, m_0, g_0, \lambda_0) = \mathcal{L}(A, q, \eta, m, g\mu^\epsilon, \lambda) + \mathcal{L}_c(A, q, \eta, m, g\mu^\epsilon, \lambda) , \quad (3.38)$$

where \mathcal{L}_c defines the counterterms. The bare and renormalised quantities are related by

$$\begin{aligned} A^\mu &= Z_3^{-\frac{1}{2}} A_0^\mu, \quad \lambda = Z_3^{-1} \lambda_0, \quad q = Z_2^{-\frac{1}{2}} q_0, \quad m = Z_m^{-1} m_0, \quad \eta = \tilde{Z}_3^{-\frac{1}{2}} \eta_0, ; \\ g_0 &= g\mu^\epsilon Z_g = g\mu^\epsilon \frac{Z_1}{Z_3^{\frac{3}{2}}} = g\mu^\epsilon \frac{\tilde{Z}_1}{\tilde{Z}_3 Z_3^{\frac{1}{2}}} = g\mu^\epsilon \frac{Z_1^F}{Z_2} = g\mu^\epsilon \frac{Z_4^{\frac{1}{2}}}{Z_3} . \end{aligned} \quad (3.39)$$

In Eq. (3.39), the renormalisation constants $Z_1, Z_1^F, \tilde{Z}_1, Z_4$ refer to the 3-gluon vertex, quark-gluon-vertex, ghost-gluon vertex and 4-gluon vertex, respectively. The counter-

term Lagrangian thus naively is given by

$$\begin{aligned}
\mathcal{L}_c = & -\frac{1}{4}(Z_3 - 1)(\partial_\mu A_\nu - \partial_\nu A_\mu)^2 + i(Z_2 - 1)\bar{q}\not{\partial}q \\
& - (Z_2 Z_m - 1)\bar{q}m q + (\tilde{Z}_3 - 1)\partial_\mu \eta^\dagger \partial^\mu \eta \\
& + \frac{g}{2}\mu^\epsilon (Z_1 - 1)f^{abc}(\partial_\mu A_\nu^a - \partial_\nu A_\mu^a)A_b^\mu A_c^\nu + (\tilde{Z}_1 - 1)ig\mu^\epsilon \partial_\mu \eta^\dagger \mathcal{A}^\mu \eta \\
& - (Z_1^F - 1)g\mu^\epsilon \bar{q}\mathcal{A}^\mu q - \frac{g^2}{4}\mu^{2\epsilon}(Z_4 - 1)f^{abc}f^{ade}A_b^\mu A_c^\nu A_d^\mu A_e^\nu.
\end{aligned} \tag{3.40}$$

However, not all the constants are independent. Otherwise we would have a problem with the renormalisation of the strong coupling constant in Eq. (3.39), because it would lead to different values for Z_g . Fortunately, we can exploit the Slavnov-Taylor identities

$$\frac{Z_1}{Z_3} = \frac{\tilde{Z}_1}{\tilde{Z}_3} = \frac{Z_1^F}{Z_2} = \frac{Z_4}{Z_1}, \tag{3.41}$$

which are generalisations of the Ward Identity $Z_1^F = Z_2$ for QED.

3.5 The running coupling and the QCD beta function

We mentioned already that the strong coupling constant, defined as $\alpha_s = g_s^2/(4\pi)$, is not really a constant. Where does the running of the coupling come from? It is closely linked to *renormalisation*, as it introduces another scale into the game, the *renormalisation scale* μ .

Let us look at a physical observable, for example the R -ratio already introduced in Section 1,

$$R(s) = \frac{\sigma(e^+e^- \rightarrow \text{hadrons})}{\sigma(e^+e^- \rightarrow \mu^+\mu^-)}. \tag{3.42}$$

We assume that the energy s exchanged in the scattering process is much larger than Λ_{QCD} , where $\Lambda_{QCD} \simeq 300 \text{ MeV}$ is the energy scale below which non-perturbative effects start to dominate, the mass scale of hadronic physics.

At leading order in perturbation theory, we have to calculate the diagram in Fig. 1 (we restrict ourselves to photon exchange, we know the result already:

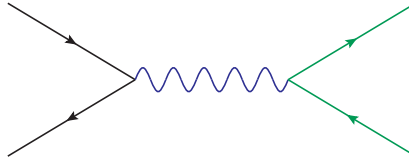


Figure 1: Leading order diagram for $e^+e^- \rightarrow f\bar{f}$.

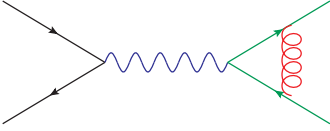
$$R(s) = N_c \sum_f Q_f^2 \theta(s - 4m_f^2) , \quad (3.43)$$

where Q_f is the electromagnetic charge of fermion f . However, we have quantum corrections where virtual gluons are exchanged, example diagrams are shown in Figs. 2a and 2b, where Fig. 2a shows corrections of order α_s (NLO), and Fig. 2b shows example diagrams for $\mathcal{O}(\alpha_s^2)$ (NNLO) corrections. The perturbative expansion for R can be written as

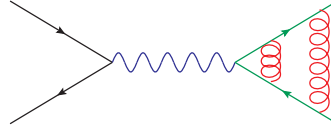
$$R(s) = K_{QCD}(s) R_0 , \quad R_0 = N_c \sum_f Q_f^2 \theta(s - 4m_f^2) ,$$

$$K_{QCD}(s) = 1 + \frac{\alpha_s(\mu^2)}{\pi} + \sum_{n \geq 2} C_n \left(\frac{s}{\mu^2} \right) \left(\frac{\alpha_s(\mu^2)}{\pi} \right)^n . \quad (3.44)$$

The higher the order in α_s the harder is the calculation. Meanwhile we know the C_n up to order α_s^4 [21, 22].



(a) 1-loop diagram contributing to $e^+e^- \rightarrow f\bar{f}$. (b) 2-loop diagram example contributing to $e^+e^- \rightarrow f\bar{f}$.



However, if we try to calculate the loop in Fig. 2a, we will encounter ultraviolet divergences. How to deal with them has been discussed in Section 3.1. We have to absorb the divergences in the bare coupling α_s^0 . For the sake of the argument we introduce an arbitrary cutoff scale Λ_{UV} for the upper integration boundary (for more complicated calculations dimensional regularisation should be used). If we carried through the calculation, we would see that the dependence on the cutoff cancels at order α_s , which is a consequence of the Ward Identities in QED. However, if we go one order higher in α_s , calculating diagrams like the one in Fig. 2b, the cutoff-dependence does not cancel anymore. We obtain

$$K_{QCD}(s) = 1 + \frac{\alpha_s}{\pi} + \left(\frac{\alpha_s}{\pi} \right)^2 \left[c + b_0 \pi \log \frac{\Lambda_{UV}^2}{s} \right] + \mathcal{O}(\alpha_s^3) . \quad (3.45)$$

It looks like our result is infinite, as we should take the limit $\Lambda_{UV} \rightarrow \infty$. However, we did not claim that α_s is the coupling we measure. It is the “bare” coupling, α_s^0 , which appears in Eq. (3.45), and we can absorb the infinity in the bare coupling to arrive at

the renormalised coupling, which is the one we measure.
In our case, this looks as follows. Define

$$\alpha_s(\mu) = \alpha_s^0 + b_0 \log \frac{\Lambda_{UV}^2}{\mu^2} \alpha_s^2, \quad (3.46)$$

then replace α_s^0 by $\alpha_s(\mu)$ and drop consistently all terms of order α_s^3 . This leads to

$$K_{QCD}^{\text{ren}}(\alpha_s(\mu), \mu^2/s) = 1 + \frac{\alpha_s(\mu)}{\pi} + \left(\frac{\alpha_s(\mu)}{\pi} \right)^2 \left[c + b_0 \pi \log \frac{\mu^2}{s} \right] + \mathcal{O}(\alpha_s^3). \quad (3.47)$$

K_{QCD}^{ren} is finite, but now it depends on the scale μ , both explicitly and through $\alpha_s(\mu)$. However, the hadronic R -ratio is a physical quantity and therefore cannot depend on the arbitrary scale μ . The dependence of K_{QCD} on μ is an artefact of the truncation of the perturbative series after the order α_s^2 .

Renormalisation group and asymptotic freedom

Since the measured hadronic R -ratio $R^{\text{ren}} = R_0 K_{QCD}^{\text{ren}}$ cannot depend μ , we know

$$\mu^2 \frac{d}{d\mu^2} R^{\text{ren}}(\alpha_s(\mu), \mu^2/Q^2) = 0 = \left(\mu^2 \frac{\partial}{\partial \mu^2} + \mu^2 \frac{\partial \alpha_s}{\partial \mu^2} \frac{\partial}{\partial \alpha_s} \right) R^{\text{ren}}(\alpha_s(\mu), \mu^2/Q^2). \quad (3.48)$$

Equation (3.48) is called *renormalisation group equation (RGE)*. Introducing the abbreviations

$$t = \ln \frac{Q^2}{\mu^2}, \quad \beta(\alpha_s) = \mu^2 \frac{\partial \alpha_s}{\partial \mu^2}, \quad (3.49)$$

the RGE becomes

$$\left(-\frac{\partial}{\partial t} + \beta(\alpha_s) \frac{\partial}{\partial \alpha_s} \right) R = 0. \quad (3.50)$$

This first order partial differential equation can be solved by implicitly defining a function $\alpha_s(Q^2)$, the *running coupling*, by

$$t = \int_{\alpha_s}^{\alpha_s(Q^2)} \frac{dx}{\beta(x)}, \quad \text{with} \quad \alpha_s \equiv \alpha_s(\mu^2), \quad (3.51)$$

where

$$\frac{\partial \alpha_s(Q^2)}{\partial t} = \beta(\alpha_s(Q^2)). \quad (3.52)$$

It is now straightforward to prove that the value of R for $\mu^2 = Q^2$, $R(1, \alpha_s(Q^2))$, solves Eq. (3.50).

Thus we have shown that the scale dependence in R enters only through $\alpha_s(Q^2)$, and that we can predict the scale dependence of R by solving Eq. (3.51), resp. the one of $\alpha_s(Q^2)$ by Eq. (3.52).

One can solve Eq. (3.52) perturbatively using an expansion of the β -function

$$\beta(\alpha_s) = -b_0 \alpha_s^2 \left[1 + \sum_{n=1}^{\infty} b_n \alpha_s^n \right] , \quad b_0 = \frac{1}{4\pi} \left(\frac{11}{3} C_A - \frac{4}{3} T_R N_f \right) . \quad (3.53)$$

The first five coefficients are known [23], where the five-loop β -function has been calculated only very recently [24–27].

If $\alpha_s(Q^2)$ is small we can truncate the series. The solution at leading-order (LO) accuracy is

$$\begin{aligned} Q^2 \frac{\partial \alpha_s}{\partial Q^2} = \frac{\partial \alpha_s}{\partial t} = -b_0 \alpha_s^2 &\Rightarrow -\frac{1}{\alpha_s(Q^2)} + \frac{1}{\alpha_s(\mu^2)} = -b_0 t \\ \Rightarrow \alpha_s(Q^2) &= \frac{\alpha_s(\mu^2)}{1 + b_0 t \alpha_s(\mu^2)} . \end{aligned} \quad (3.54)$$

Eq. (3.54) implies that

$$\alpha_s(Q^2) \xrightarrow{Q^2 \rightarrow \infty} \frac{1}{b_0 t} \xrightarrow{Q^2 \rightarrow \infty} 0 . \quad (3.55)$$

Now we see the behaviour leading to *asymptotic freedom*: the larger Q^2 , the smaller the coupling, so at very high energies (small distances), the quarks and gluons can be treated as if they were free particles. The behaviour of α_s as a function of Q^2 is illustrated in Fig. 3 including recent measurements.

Note that $b_0 > 0$ for $N_f < 11/2 C_A$ (see Eq. (3.53)), so b_0 is positive for QCD (while it is negative for QED). It can be proven that, in 4 space-time dimensions, only non-Abelian gauge theories can be asymptotically free. For the discovery of asymptotic freedom in QCD [28, 29], Gross, Politzer and Wilczek got the Nobel Prize in 2004.

In the derivation of the RGE above, we have assumed that the observable R does not depend on other mass scales like quark masses. However, the renormalisation group equations can be easily extended to include mass renormalisation, which will lead to running quark masses:

$$\left(\mu^2 \frac{\partial}{\partial \mu^2} + \beta(\alpha_s) \frac{\partial}{\partial \alpha_s} - \gamma_m(\alpha_s) m \frac{\partial}{\partial m} \right) R \left(\frac{Q^2}{\mu^2}, \alpha_s, \frac{m}{Q} \right) = 0 , \quad (3.56)$$

where γ_m is called the mass anomalous dimension and the minus sign before γ_m is a convention. In a perturbative expansion we can write the mass anomalous dimension as $\gamma_m(\alpha_s) = c_0 \alpha_s (1 + \sum_n c_n \alpha_s^n)$. The coefficients are known up to c_4 [30, 31].

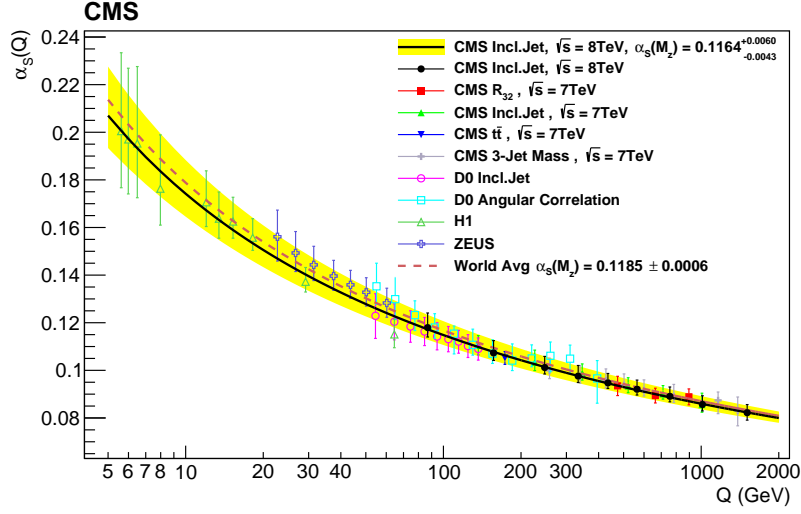


Figure 3: The running coupling $\alpha_s(Q^2)$. *Figure from arXiv:1609.05331.*

The β -function in D dimensions

As we saw already, the running of α_s is a consequence of the renormalisation scale independence of physical observables. The bare coupling g_0 knows nothing about our choice of μ . Therefore we must have

$$\frac{dg_0}{d\mu} = 0. \quad (3.57)$$

Using the definition

$$g_0 = g\mu^\epsilon Z_g \quad (3.58)$$

we obtain

$$\mu^{2\epsilon} \left(\epsilon Z_g \alpha_s + 2\alpha_s \frac{dZ_g}{dt} + Z_g \frac{d\alpha_s}{dt} \right) = 0, \quad (3.59)$$

where $\frac{d}{dt} = \mu^2 \frac{d}{d\mu^2} = \frac{d}{d \ln \mu^2}$. Z_g depends upon μ only through α_s (at least in the $\overline{\text{MS}}$ scheme). Using $\beta(\alpha_s) = \frac{d\alpha_s}{dt}$ we obtain

$$\beta(\alpha_s) + 2\alpha_s \frac{1}{Z_g} \frac{dZ_g}{d\alpha_s} \beta(\alpha_s) = -\epsilon \alpha_s. \quad (3.60)$$

Now we expand Z_g as

$$Z_g = 1 - \frac{1}{\epsilon} \frac{b_0}{2} \alpha_s + \mathcal{O}(\alpha_s^2) \quad (3.61)$$

and obtain

$$\beta(\alpha_s) = -\epsilon \alpha_s \frac{1}{1 - \frac{b_0 \alpha_s}{\epsilon}} = -b_0 \alpha_s^2 + \mathcal{O}(\alpha_s^3, \epsilon). \quad (3.62)$$

This means that the β -function can be obtained from the coefficient of the single pole of Z_g . In fact, in the $\overline{\text{MS}}$ scheme, this remains even true beyond one-loop.

Scale uncertainties

From the perturbative solution of the RGE we can derive how a physical quantity $O^{(N)}(\mu)$, expanded in α_s as $O^{(N)}(\mu) = \sum_n^N c_n(\mu) \alpha_s(\mu^2)^n$ and truncated at order N in perturbation theory, changes with the renormalisation scale μ :

$$\frac{d}{d \log(\mu^2)} O^{(N)}(\mu) \sim \mathcal{O}(\alpha_s(\mu^2)^{N+1}) . \quad (3.63)$$

Therefore it is clear that, the more higher order coefficients c_n we can calculate, the less our result will depend on the unphysical scale μ^2 . An example is shown in Fig. 4.

In hadronic collisions there is another scale, the factorisation scale μ_F , which needs to be taken into account when assessing the uncertainty of the theoretical prediction.

3.6 NLO calculations and infrared singularities

3.6.1 Structure of NLO calculations

Next-to-leading order calculations consist of several parts, which can be classified as virtual corrections (containing usually one loop), real corrections (radiation of extra particles relative to leading order) and subtraction terms. In the following we will assume that the virtual corrections already include UV renormalisation, such that the subtraction terms only concern the subtraction of the infrared (IR, soft and collinear) singularities. We will consider “NLO” as next-to-leading order in an expansion in the strong coupling constant, even though the general structure is very similar for electroweak corrections. The real and virtual contributions to the simple example $\gamma^* \rightarrow q\bar{q}$ are shown in Fig. 5.

If \mathcal{M}_0 is the leading order amplitude (also called *Born* amplitude) and $\mathcal{M}_{\text{virt}}, \mathcal{M}_{\text{real}}$ are the virtual and real amplitudes as shown in Fig. 5, the corresponding cross section

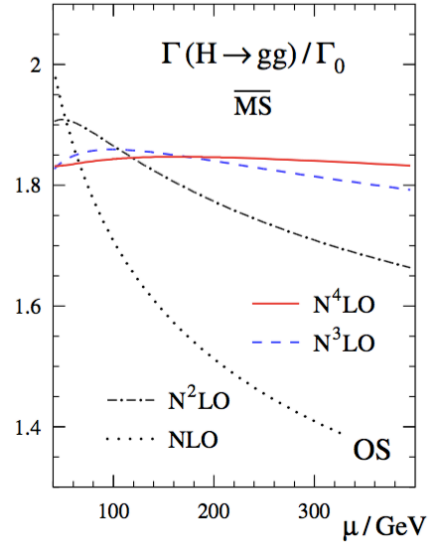


Figure 4: Example $H \rightarrow gg$ for the reduction of the scale dependence at higher orders. *Figure from Ref. [22].*

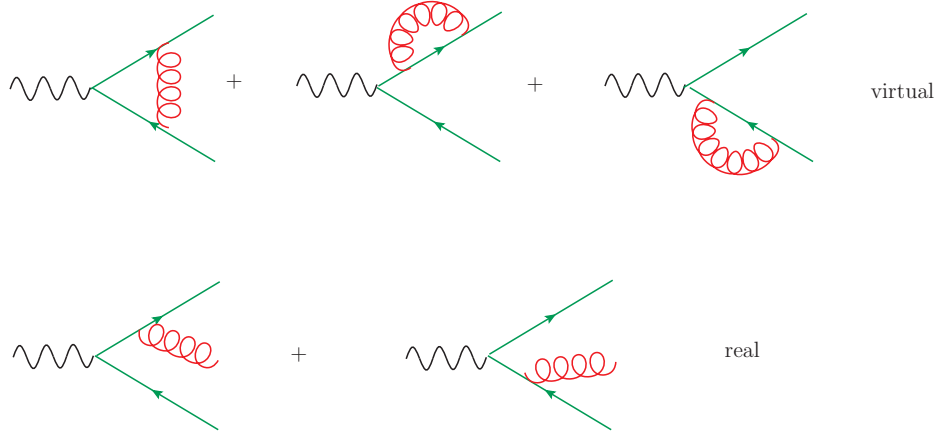


Figure 5: The real and virtual contributions to $\gamma^* \rightarrow q\bar{q}$ at order α_s .

is given by

$$\sigma^{NLO} = \underbrace{\int d\phi_2 |\mathcal{M}_0|^2}_{\sigma^{LO}} + \int_R d\phi_3 |\mathcal{M}_{\text{real}}|^2 + \int_V d\phi_2 2\text{Re}(\mathcal{M}_{\text{virt}}\mathcal{M}_0^*) . \quad (3.64)$$

The sum of the integrals \int_R and \int_V above is finite. However, this is not true for the individual contributions. The real part contains divergences due to soft and collinear radiation of massless particles. While $\mathcal{M}_{\text{real}}$ itself is a tree level amplitude and thus finite, the divergences show up upon integration over the phase space $d\Phi_3$. In \int_V , the phase space is the same as for the *Born* amplitude, but the loop integrals contained in $\mathcal{M}_{\text{virt}}$ contain IR singularities.

Let us anticipate the answer, which we will (partly) calculate later. We find:

$$\begin{aligned} \sigma_R &= \sigma^{\text{Born}} H(\epsilon) C_F \frac{\alpha_s}{2\pi} \left(\frac{2}{\epsilon^2} + \frac{3}{\epsilon} + \frac{19}{2} - \pi^2 \right) , \\ \sigma_V &= \sigma^{\text{Born}} H(\epsilon) C_F \frac{\alpha_s}{2\pi} \left(-\frac{2}{\epsilon^2} - \frac{3}{\epsilon} - 8 + \pi^2 \right) , \end{aligned} \quad (3.65)$$

where $H(\epsilon) = 1 + \mathcal{O}(\epsilon)$, and the exact form is irrelevant here, because the poles in ϵ all cancel! This must be the case according to the KLN (Kinoshita-Lee-Nauenberg) theorem [32, 33]. It says that *IR singularities must cancel when summing the transition rate over all degenerate (initial and final) states*. In our example, we do not have initial state singularities. However, in the final state we can have massless quarks accompanied by soft and/or collinear gluons (resp. just one extra gluon at order α_s). Such a state cannot be distinguished from just a quark state, and therefore is degenerate. Only when

summing over all the final state multiplicities (at each order in α_s), the divergences cancel. Another way of stating this is looking at the squared amplitude at order α_s and considering all cuts, see Fig. 6 (contributions which are zero for massless quarks are not shown). The KLN theorem states that the sum of all cuts leading to physical final states is free of IR poles.

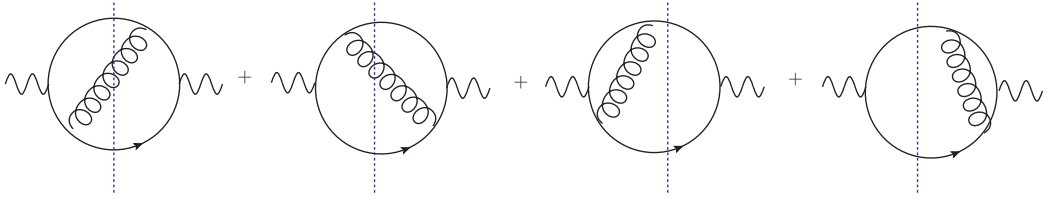


Figure 6: The sum over cuts of the amplitude squared shown above is finite according to the KLN theorem.

Remember from eq. (2.14) that the general formula to obtain a cross section from the amplitude is given by

$$d\sigma = \frac{S}{\text{flux}} \bar{\Sigma} |\mathcal{M}|^2 d\Phi . \quad (3.66)$$

Note that the flux factor for two massless initial state particles (e.g. in $e^+e^- \rightarrow \text{hadrons}$) is just $4 p_1 \cdot p_2 = 2 \hat{s}$.

The cancellations between \int_R and \int_V in Eq. (3.64) are highly non-trivial, because the phase space integrals contain a different number of particles in the final state. If we want to calculate a prediction for a certain observable, we need to multiply the amplitude by a *measurement function* $J(p_1 \dots p_n)$ containing for example a jet definition, acting on the n particles in the final state. Schematically, the structure of the cross section then is the following. Let us consider the case where we have an IR pole if the variable x , denoting for example the energy of an extra gluon in the real radiation part, goes to zero. If we define

$$\begin{aligned} \mathcal{B}_n &= \int d\phi_n |\mathcal{M}_0|^2 = \int d\phi_n B_n \\ \mathcal{V}_n &= \int d\phi_n 2 \text{Re} (\mathcal{M}_{\text{virt}} \mathcal{M}_0^*) = \int d\phi_n \frac{V_n}{\epsilon} \\ \mathcal{R}_n &= \int d\phi_{n+1} |\mathcal{M}_{\text{real}}|^2 = \int d\phi_n \int_0^1 dx x^{-1-\epsilon} R_n(x) \end{aligned} \quad (3.67)$$

and a measurement function $J(p_1 \dots p_n, x)$ we have

$$\sigma^{NLO} = \int d\phi_n \left\{ \left(B_n + \frac{V_n}{\epsilon} \right) J(p_1 \dots p_n, 0) + \int_0^1 dx x^{-1-\epsilon} R_n(x) J(p_1 \dots p_n, x) \right\} . \quad (3.68)$$

The cancellation of the pole in $\frac{V_n}{\epsilon}$ by the integral over $R_n(x)$ will only work if

$$\lim_{x \rightarrow 0} J(p_1 \dots p_n, x) = J(p_1 \dots p_n, 0) . \quad (3.69)$$

This is a non-trivial condition for the definition of an observable, for example a jet algorithm, and is called *infrared safety*. Note that the measurement function is also important if we define differential cross sections $d\sigma/dX$ (also called distributions), for example the transverse momentum distribution $d\sigma/dp_T$ of one of the final state particles. In this case we have $J(p_1 \dots p_n) = \delta(X - \chi_n(p_i))$, where $\chi_n(p_i)$ is the definition of the observable, based on n partons. Again, infrared safety requires $\chi_{n+1}(p_i) \rightarrow \chi_n$ if one of the p_i becomes soft or two of the momenta become collinear to each other, see below.

3.6.2 Soft gluon emission and collinear singularities

For this part please have a look at the Monte Carlo lectures by Johannes Bellm.

3.6.3 Phase space integrals in D dimensions

The general formula for a $1 \rightarrow n$ particle phase space $d\Phi_n$ with $Q \rightarrow p_1 \dots p_n$ is given by

$$d\Phi_{1 \rightarrow n} = (2\pi)^{n-D(n-1)} \left[\prod_{j=1}^n d^D p_j \delta(p_j^2 - m_j^2) \Theta(E_j) \right] \delta\left(Q - \sum_{j=1}^n p_j\right) . \quad (3.70)$$

In the following we will stick to the massless case $m_j = 0$. We use

$$d^D p_j \delta(p_j^2) \Theta(E_j) = dE_j d^{D-1} \vec{p}_j \delta(E_j^2 - \vec{p}_j^2) \Theta(E_j) = \frac{1}{2E_j} d^{D-1} \vec{p}_j \Big|_{E_j=|\vec{p}_j|} \quad (3.71)$$

for $j = 1, \dots, n-1$ to arrive at

$$d\Phi_{1 \rightarrow n} = (2\pi)^{n-D(n-1)} 2^{1-n} \prod_{j=1}^{n-1} \frac{d^{D-1} \vec{p}_j}{|\vec{p}_j|} \delta\left((Q - \sum_{j=1}^{n-1} p_j)^2\right) , \quad (3.72)$$

where we have used the last δ -function in Eq. (3.70) to eliminate p_n . We further use

$$\frac{d^{D-1} \vec{p}}{|\vec{p}|} f(|\vec{p}|) = d\Omega_{D-2} d|\vec{p}| |\vec{p}|^{D-3} f(|\vec{p}|) , \quad (3.73)$$

$$\begin{aligned} \int d\Omega_{D-2} &= \int d\Omega_{D-3} \int_0^\pi d\theta (\sin \theta)^{D-3} = \int_0^\pi d\theta_1 (\sin \theta_1)^{D-3} \int_0^\pi d\theta_2 (\sin \theta_2)^{D-4} \dots \int_0^{2\pi} d\theta \\ \int_{S_{D-2}} d\Omega_{D-2} &= V(D-1) = \frac{2\pi^{\frac{D-1}{2}}}{\Gamma(\frac{D-1}{2})} , \end{aligned}$$

to obtain

$$d\Phi_{1 \rightarrow n} = (2\pi)^{n-D(n-1)} 2^{1-n} d\Omega_{D-2} \prod_{j=1}^{n-1} d|\vec{p}_j| |\vec{p}_j|^{D-3} \delta\left((Q - \sum_{j=1}^{n-1} p_j)^2\right). \quad (3.74)$$

Example 1 \rightarrow 2:

For $n = 2$ the momenta can be parametrised by

$$Q = (E, \vec{0}^{(D-1)}) , \quad p_1 = E_1 (1, \vec{0}^{(D-2)}, 1) , \quad p_2 = Q - p_1 . \quad (3.75)$$

Integrating out the δ -distribution leads to

$$d\Phi_{1 \rightarrow 2} = (2\pi)^{2-D} 2^{1-D} (Q^2)^{D/2-2} d\Omega_{D-2} . \quad (3.76)$$

Example 1 \rightarrow 3:

For $n = 3$ one can choose a coordinate frame such that

$$\begin{aligned} Q &= (E, \vec{0}^{(D-1)}) \\ p_1 &= E_1 (1, \vec{0}^{(D-2)}, 1) \\ p_2 &= E_2 (1, \vec{0}^{(D-3)}, \sin \theta, \cos \theta) \\ p_3 &= Q - p_2 - p_1 , \end{aligned} \quad (3.77)$$

leading to

$$\begin{aligned} d\Phi_{1 \rightarrow 3} &= \frac{1}{4} (2\pi)^{3-2D} dE_1 dE_2 d\theta_1 (E_1 E_2 \sin \theta)^{D-3} d\Omega_{D-2} d\Omega_{D-3} \\ &\quad \Theta(E_1) \Theta(E_2) \Theta(E - E_1 - E_2) \delta((Q - p_1 - p_2)^2) . \end{aligned} \quad (3.78)$$

In the following a parametrisation in terms of the Mandelstam variables $s_{ij} = 2p_i \cdot p_j$ will be useful, therefore we make the transformation $E_1, E_2, \theta \rightarrow s_{12}, s_{23}, s_{13}$. To work with dimensionless variables we define $y_1 = s_{12}/Q^2$, $y_2 = s_{13}/Q^2$, $y_3 = s_{23}/Q^2$ which leads to

$$\begin{aligned} d\Phi_{1 \rightarrow 3} &= (2\pi)^{3-2D} 2^{-1-D} (Q^2)^{D-3} d\Omega_{D-2} d\Omega_{D-3} (y_1 y_2 y_3)^{D/2-2} \\ &\quad dy_1 dy_2 dy_3 \Theta(y_1) \Theta(y_2) \Theta(y_3) \delta(1 - y_1 - y_2 - y_3) . \end{aligned} \quad (3.79)$$

Now we are in the position to calculate the full real radiation contribution. The matrix element (for one quark flavour with charge Q_f) in the variables defined above, where p_3 in our case is the gluon, is given by

$$|\mathcal{M}|_{\text{real}}^2 = C_F e^2 Q_f^2 g_s^2 8(1 - \epsilon) \left\{ \frac{2}{y_2 y_3} + \frac{-2 + (1 - \epsilon)y_3}{y_2} + \frac{-2 + (1 - \epsilon)y_2}{y_3} - 2\epsilon \right\} . \quad (3.80)$$

In our variables, soft singularities mean gluon momentum $p_3 \rightarrow 0$ and therefore both y_2 and $y_3 \rightarrow 0$. While $p_3 \parallel p_1$ means $y_2 \rightarrow 0$ and $p_3 \parallel p_2$ means $y_3 \rightarrow 0$. Combined with the factors $(y_2 y_3)^{D/2-2}$ from the phase space it is clear that the first term in the bracket of Eq. (3.80) will lead to a $1/\epsilon^2$ pole, coming from the region in phase space where soft and collinear limits coincide. To eliminate the δ -distribution, we make the substitutions

$$y_1 = 1 - z_1, y_2 = z_1 z_2, y_3 = z_1(1 - z_2) \quad , \quad \det J = z_1$$

to arrive at

$$\int d\Phi_3 |\mathcal{M}|_{\text{real}}^2 = \alpha C_F \frac{\alpha_s}{\pi} Q_f^2 \tilde{H}(\epsilon) (Q^2)^{1-2\epsilon} \int_0^1 dz_1 \int_0^1 dz_2 z_1^{-2\epsilon} \left(z_2(1 - z_1)(1 - z_2) \right)^{-\epsilon} \left\{ \frac{2}{z_1 z_2(1 - z_2)} + \frac{-2 + (1 - \epsilon)z_1(1 - z_2)}{z_2} + \frac{-2 + (1 - \epsilon)z_1 z_2}{1 - z_2} - 2\epsilon z_1 \right\} . \quad (3.81)$$

The integrals can be expressed in terms of Euler Beta-functions and lead to the result quoted in Eq. (3.65).

3.6.4 Jet cross sections

Jets can be pictured as clusters of particles (usually hadrons) which are close to each other in phase space, resp. in the detector. Fig. 7 illustrates what happens between the partonic interaction and the hadrons seen in the detector.

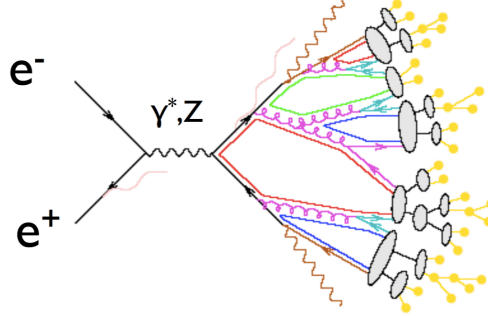


Figure 7: Parton branching and hadronisation in e^+e^- annihilation to hadrons. Figure by Fabio Maltoni.

Historically, one of the first suggestions to define jet cross sections was by Sterman and Weinberg [34]. In their definition, a final state is classified as two-jet-like if all but a fraction ϵ of the total available energy E is contained in two cones of opening angle δ . The two-jet cross section is then obtained by integrating the matrix elements

for the various quark and gluon final states over the appropriate region of phase space determined by ε and δ .

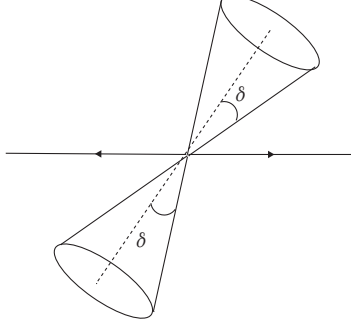


Figure 8: Two jet cones according to the definition of Sterman and Weinberg.

Let us have a look at the different contributions to the 2-jet cross section at $\mathcal{O}(\alpha_s)$, see Fig. 9.

- (a) The Born contribution σ_0 . As we have only two partons, this is always a 2-jet configuration, no matter what the values for ε and δ are.
- (b) The virtual contribution

$$\sigma^V = -\sigma_0 C_F \frac{\alpha_s}{2\pi} 4 \int_0^E \frac{dk_0}{k_0} \frac{d \cos \theta}{(1 - \cos \theta)(1 + \cos \theta)} .$$

- (c) The soft contribution ($k_0 < \varepsilon E$):

$$\sigma^{\text{soft}} = \sigma_0 C_F \frac{\alpha_s}{2\pi} 4 \int_0^{\varepsilon E} \frac{dk_0}{k_0} \frac{d \cos \theta}{(1 - \cos \theta)(1 + \cos \theta)} .$$

- (d) The collinear contribution ($k_0 > \varepsilon E, \theta < \delta$):

$$\sigma^{\text{coll}} = \sigma_0 C_F \frac{\alpha_s}{2\pi} 4 \int_{\varepsilon E}^E \frac{dk_0}{k_0} \left(\int_0^\delta + \int_{\pi-\delta}^\pi \right) \frac{d \cos \theta}{(1 - \cos \theta)(1 + \cos \theta)} .$$

Summing up all these contributions leads to

$$\begin{aligned} \sigma^{2jet} &= \sigma_0 \left(1 - C_F \frac{\alpha_s}{2\pi} 4 \int_{\varepsilon E}^E \frac{dk_0}{k_0} \int_\delta^{\pi-\delta} \frac{d \cos \theta}{(1 - \cos^2 \theta)} \right) \\ &= \sigma_0 \left(1 - 4 C_F \frac{\alpha_s}{2\pi} \ln \varepsilon \ln \delta \right) . \end{aligned} \tag{3.82}$$

Of course the two-jet cross section depends on the values for ε and δ . If they are

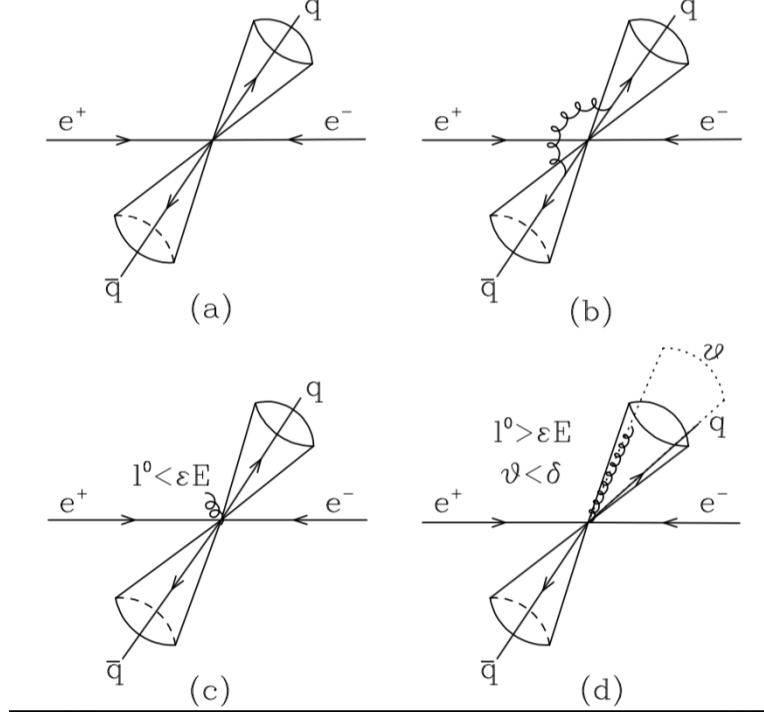


Figure 9: Different configurations contributing to the 2-jet cross section at $\mathcal{O}(\alpha_s)$.

very large, even extra radiation at a relatively large angle $\theta < \delta$ will be “clustered” into the jet cone and almost all events will be classified as 2-jet events. Note that the partonic 3-jet cross section at $\mathcal{O}(\alpha_s)$ is given by $\sigma^{3jet} = \sigma_{NLO}^{total} - \sigma^{2jet}$, because from the theory point of view, we cannot have more than 3 partons at NLO in the process $e^+e^- \rightarrow hadrons$. In the experiment of course we can have more jets, which come from parton branchings (“parton shower”) before the process of hadronisation. Fig. 10 shows that it is not obvious how many events are identified as 2-jet (or 3-jet, 4-jet, ...) events after parton showering and hadronisation. This depends on the jet algorithm used to identify the jets. It is clear from Fig. 10 that a lot of information is lost when projecting a complex hadronic track structure onto an n -jet event. Modern techniques also identify a *jet substructure*, in particular for highly energetic jets. This can give valuable information on the underlying partonic event (e.g. distinguishing a gluon from a quark, a b -quark from a light quark, etc).

The Stermann-Weinberg jet definition based on cones is not very practical to analyse multijet final states. A better alternative is for example the following:

1. starting from n particles, for all pairs i and j calculate $(p_i + p_j)^2$.
2. If $\min(p_i + p_j)^2 < y_{cut} Q^2$ then define a new “pseudo-particle” $p_J = p_i + p_j$, which

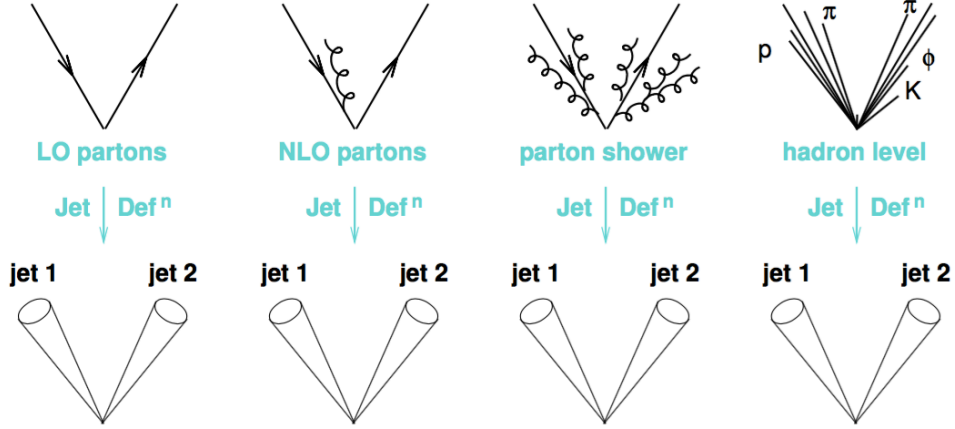


Figure 10: Projections to a 2-jet event at various stages of the theoretical description. Figure by Gavin Salam.

decreases $n \rightarrow n - 1$. Q is the center-of-mass energy, y_{cut} is the jet resolution parameter.

3. if $n = 1$ stop, else repeat the step above.

It is evident that a large value of y_{cut} will ultimately result in the clustering all particles into only two jets, while higher jet multiplicities will become more and more frequent as y_{cut} is lowered. After this algorithm all partons are clustered into jets. With the above definition one finds at $\mathcal{O}(\alpha_s)$:

$$\sigma^{2jet} = \sigma_0 \left(1 - C_F \frac{\alpha_s}{\pi} \ln^2 y_{\text{cut}} \right) . \quad (3.83)$$

Algorithms which are particularly useful for hadronic initial states are for example the so-called Durham- k_T algorithm [35] or the anti- k_T algorithm [36] (see also [37] for a summary of different jet algorithms).

The Durham- k_T -jet algorithm clusters particles into jets by computing the distance measure

$$y_{ij,D} = \frac{2 \min(E_i^2, E_j^2)(1 - \cos \theta_{ij})}{Q^2} \quad (3.84)$$

for each pair (i, j) of particles. Q is the center-of-mass energy. The pair with the lowest $y_{ij,D}$ is replaced by a pseudo-particle whose four-momentum is given by the sum of the four-momenta of particles i and j ('E' recombination scheme). This procedure is repeated as long as pairs with invariant mass below the predefined resolution parameter $y_{ij,D} < y_{\text{cut}}$ are found. Once the clustering is terminated, the remaining (pseudo)-particles are the jets.

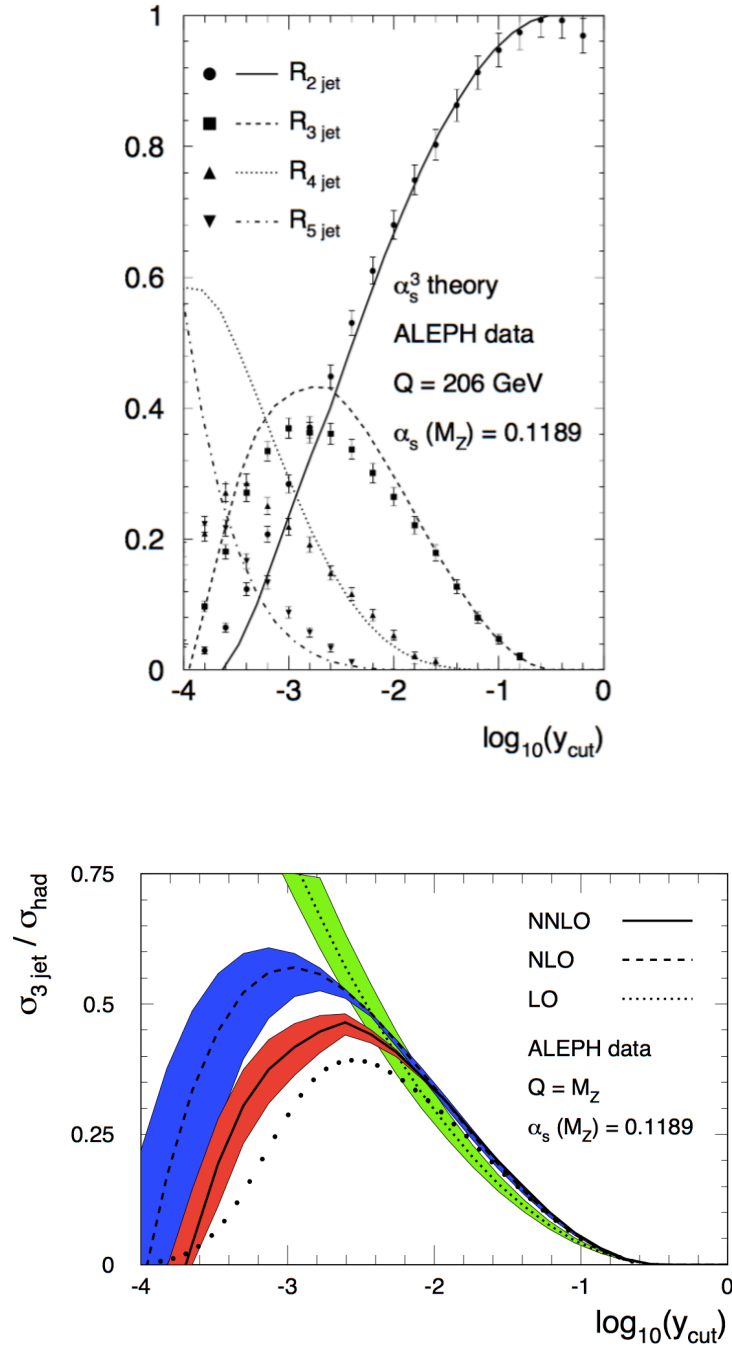


Figure 11: Jet rates as a function of the jet resolution parameter y_{cut} (upper figure) and higher order corrections to the 3-jet rate from Ref. [38] (lower figure).

Fig. 11 (a) shows the jet rates (normalised to the total hadronic cross section) as a function of y_{cut} , compared to ALEPH data. Fig. 11 (b) shows corrections up to NNLO to the 3-jet rate as a function of y_{cut} . Note that for small values of y_{cut} the 2-jet rate diverges $\sim -\log^2(y_{\text{cut}})$ because only three partons are present at LO.

At the LHC, the most commonly used jet algorithm is the *anti- k_T algorithm* [36]. The anti- k_T algorithm is similar to the Durham- k_T algorithm, but introduces a different distance measure:

$$y_{ij,a} = \frac{1}{8} Q^2 \min \left(\frac{1}{E_i^2}, \frac{1}{E_j^2} \right) (1 - \cos \theta_{ij}) \quad (3.85)$$

Since very recently, methods based on *Deep Learning* are applied to identify jets, and seem to be quite successful.

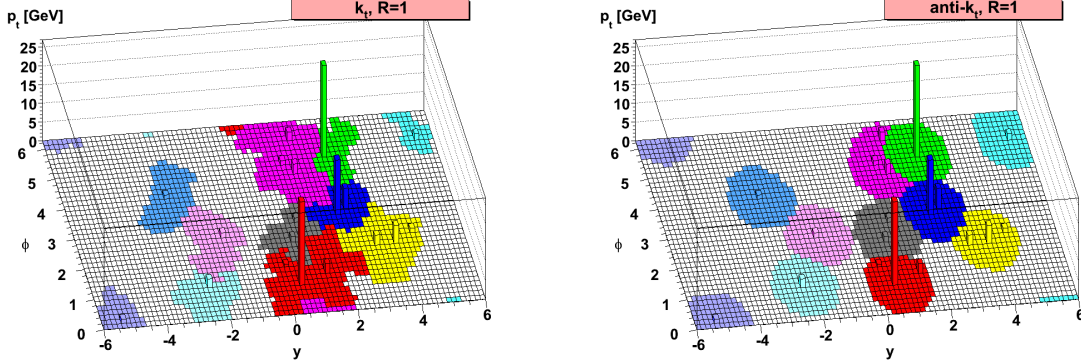


Figure 12: Jet areas as a result of (a) the Durham- k_T algorithm, (b) the anti- k_T algorithm. Figures from Ref. [36].

Of course, jets are not the only observables one can define based on hadronic tracks in the detector. Another very useful observable is *thrust*, which describes how “pencil-like” an event looks like. Thrust is an example of so-called *event-shape* observables. Thrust T is defined by

$$T = \max_{\vec{n}} \frac{\sum_{i=1}^m |\vec{p}_i \cdot \vec{n}|}{\sum_{i=1}^m |\vec{p}_i|}, \quad (3.86)$$

where \vec{n} is a three-vector (the direction of the thrust axis) such that T is maximal. The particle three-momenta \vec{p}_i are defined in the e^+e^- centre-of-mass frame. T is an example of a jet function $J(p_1, \dots, p_m)$. It is infrared safe because neither $p_j \rightarrow 0$, nor replacing p_i with $zp_i + (1-z)p_i$ change T .

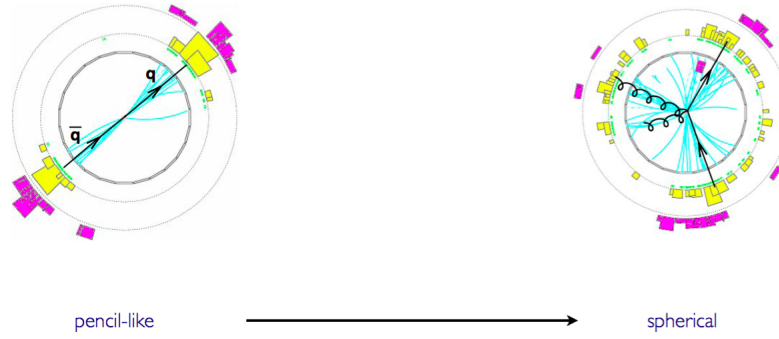


Figure 13: The thrust event shape ranges from “pencil-like” to “spherical”. Figure: Fabio Maltoni.

3.7 Parton distribution functions

Parton distribution functions (PDFs) will be introduced in the MC lecture by Johannes Bellm.

References

- [1] G. 't Hooft and M. J. G. Veltman, *Regularization and Renormalization of Gauge Fields*, *Nucl. Phys.* **B44** (1972) 189–213.
- [2] C. G. Bollini and J. J. Giambiagi, *Dimensional Renormalization: The Number of Dimensions as a Regularizing Parameter*, *Nuovo Cim.* **B12** (1972) 20–26.
- [3] P. Breitenlohner and D. Maison, *Dimensional Renormalization and the Action Principle*, *Commun. Math. Phys.* **52** (1977) 11–38.
- [4] S. A. Larin, *The Renormalization of the axial anomaly in dimensional regularization*, *Phys. Lett.* **B303** (1993) 113–118, [[hep-ph/9302240](#)].
- [5] S. Catani, M. H. Seymour and Z. Trocsanyi, *Regularization scheme independence and unitarity in QCD cross-sections*, *Phys. Rev.* **D55** (1997) 6819–6829, [[hep-ph/9610553](#)].
- [6] A. Signer and D. Stöckinger, *Using Dimensional Reduction for Hadronic Collisions*, *Nucl. Phys.* **B808** (2009) 88–120, [[0807.4424](#)].
- [7] T. Binoth, J. P. Guillet, G. Heinrich, E. Pilon and C. Schubert, *An Algebraic/numerical formalism for one-loop multi-leg amplitudes*, *JHEP* **10** (2005) 015, [[hep-ph/0504267](#)].
- [8] T. Binoth, J. P. Guillet and G. Heinrich, *Reduction formalism for dimensionally regulated one loop N point integrals*, *Nucl. Phys.* **B572** (2000) 361–386, [[hep-ph/9911342](#)].

- [9] G. Passarino and M. J. G. Veltman, *One Loop Corrections for $e^+ e^-$ Annihilation Into $\mu^+ \mu^-$ in the Weinberg Model*, *Nucl. Phys.* **B160** (1979) 151–207.
- [10] T. Hahn, *Feynman Diagram Calculations with FeynArts, FormCalc, and LoopTools*, *PoS ACAT2010* (2010) 078, [[1006.2231](#)].
- [11] T. Hahn and M. Perez-Victoria, *Automatized one loop calculations in four-dimensions and D-dimensions*, *Comput. Phys. Commun.* **118** (1999) 153–165, [[hep-ph/9807565](#)].
- [12] A. van Hameren, *OneLoop: For the evaluation of one-loop scalar functions*, *Comput. Phys. Commun.* **182** (2011) 2427–2438, [[1007.4716](#)].
- [13] J. P. Guillet, G. Heinrich and J. F. von Soden-Fraunhofen, *Tools for NLO automation: extension of the golem95C integral library*, *Comput. Phys. Commun.* **185** (2014) 1828–1834, [[1312.3887](#)].
- [14] G. Cullen, J. P. Guillet, G. Heinrich, T. Kleinschmidt, E. Pilon, T. Reiter et al., *Golem95C: A library for one-loop integrals with complex masses*, *Comput. Phys. Commun.* **182** (2011) 2276–2284, [[1101.5595](#)].
- [15] T. Binoth, J. P. Guillet, G. Heinrich, E. Pilon and T. Reiter, *Golem95: A Numerical program to calculate one-loop tensor integrals with up to six external legs*, *Comput. Phys. Commun.* **180** (2009) 2317–2330, [[0810.0992](#)].
- [16] A. Denner, S. Dittmaier and L. Hofer, *Collier: a fortran-based Complex One-Loop Library in Extended Regularizations*, *Comput. Phys. Commun.* **212** (2017) 220–238, [[1604.06792](#)].
- [17] H. H. Patel, *Package-X: A Mathematica package for the analytic calculation of one-loop integrals*, *Comput. Phys. Commun.* **197** (2015) 276–290, [[1503.01469](#)].
- [18] S. Carrazza, R. K. Ellis and G. Zanderighi, *QCDLoop: a comprehensive framework for one-loop scalar integrals*, *Comput. Phys. Commun.* **209** (2016) 134–143, [[1605.03181](#)].
- [19] R. K. Ellis and G. Zanderighi, *Scalar one-loop integrals for QCD*, *JHEP* **02** (2008) 002, [[0712.1851](#)].
- [20] R. K. Ellis, Z. Kunszt, K. Melnikov and G. Zanderighi, *One-loop calculations in quantum field theory: from Feynman diagrams to unitarity cuts*, *Phys. Rept.* **518** (2012) 141–250, [[1105.4319](#)].
- [21] P. A. Baikov, K. G. Chetyrkin, J. H. Kühn and J. Rittinger, *Complete $\mathcal{O}(\alpha_s^4)$ QCD Corrections to Hadronic Z-Decays*, *Phys. Rev. Lett.* **108** (2012) 222003, [[1201.5804](#)].
- [22] F. Herzog, B. Ruijl, T. Ueda, J. A. M. Vermaseren and A. Vogt, *On Higgs decays to hadrons and the R-ratio at N^4 LO*, *JHEP* **08** (2017) 113, [[1707.01044](#)].
- [23] T. van Ritbergen, J. A. M. Vermaseren and S. A. Larin, *The Four loop beta function in quantum chromodynamics*, *Phys. Lett.* **B400** (1997) 379–384, [[hep-ph/9701390](#)].

- [24] P. A. Baikov, K. G. Chetyrkin and J. H. Kühn, *Five-Loop Running of the QCD coupling constant*, *Phys. Rev. Lett.* **118** (2017) 082002, [[1606.08659](#)].
- [25] F. Herzog, B. Ruijl, T. Ueda, J. A. M. Vermaseren and A. Vogt, *The five-loop beta function of Yang-Mills theory with fermions*, *JHEP* **02** (2017) 090, [[1701.01404](#)].
- [26] T. Luthe, A. Maier, P. Marquard and Y. Schröder, *The five-loop Beta function for a general gauge group and anomalous dimensions beyond Feynman gauge*, *JHEP* **10** (2017) 166, [[1709.07718](#)].
- [27] K. G. Chetyrkin, G. Falcioni, F. Herzog and J. A. M. Vermaseren, *Five-loop renormalisation of QCD in covariant gauges*, *JHEP* **10** (2017) 179, [[1709.08541](#)].
- [28] D. J. Gross and F. Wilczek, *Ultraviolet Behavior of Nonabelian Gauge Theories*, *Phys. Rev. Lett.* **30** (1973) 1343–1346.
- [29] H. D. Politzer, *Reliable Perturbative Results for Strong Interactions?*, *Phys. Rev. Lett.* **30** (1973) 1346–1349.
- [30] P. A. Baikov, K. G. Chetyrkin and J. H. Kühn, *Quark Mass and Field Anomalous Dimensions to $\mathcal{O}(\alpha_s^5)$* , *JHEP* **10** (2014) 076, [[1402.6611](#)].
- [31] P. A. Baikov, K. G. Chetyrkin and J. H. Kühn, *Five-loop fermion anomalous dimension for a general gauge group from four-loop massless propagators*, *JHEP* **04** (2017) 119, [[1702.01458](#)].
- [32] T. Kinoshita, *Mass singularities of Feynman amplitudes*, *J. Math. Phys.* **3** (1962) 650–677.
- [33] T. D. Lee and M. Nauenberg, *Degenerate Systems and Mass Singularities*, *Phys. Rev.* **133** (1964) B1549–B1562.
- [34] G. F. Sterman and S. Weinberg, *Jets from Quantum Chromodynamics*, *Phys. Rev. Lett.* **39** (1977) 1436.
- [35] S. Bethke, Z. Kunszt, D. E. Soper and W. J. Stirling, *New jet cluster algorithms: Next-to-leading order QCD and hadronization corrections*, *Nucl. Phys.* **B370** (1992) 310–334.
- [36] M. Cacciari, G. P. Salam and G. Soyez, *The Anti- $k(t)$ jet clustering algorithm*, *JHEP* **04** (2008) 063, [[0802.1189](#)].
- [37] S. Weinzierl, *Jet algorithms in electron-positron annihilation: Perturbative higher order predictions*, *Eur. Phys. J.* **C71** (2011) 1565, [[1011.6247](#)].
- [38] A. Gehrmann-De Ridder, T. Gehrmann, E. W. N. Glover and G. Heinrich, *Jet rates in electron-positron annihilation at $\mathcal{O}(\alpha(s)^{**3})$ in QCD*, *Phys. Rev. Lett.* **100** (2008) 172001, [[0802.0813](#)].